Dynamic behavior of combustion instability in a cylindrical combustor with an off-center installed coaxial injector

Haruki Kasuya, Hiroshi Gotoda, Seiji Yoshida, and Shigeru Tachibana

Citation: Chaos **28**, 033111 (2018); doi: 10.1063/1.5025480
View online: https://doi.org/10.1063/1.5025480
View Table of Contents: http://aip.scitation.org/toc/cha/28/3
Published by the American Institute of Physics

Dynamic behavior of combustion instability in a cylindrical combustor with an off-center installed coaxial injector

Haruki Kasuya,[1] Hiroshi Gotoda,[1,a)] Seiji Yoshida,[2] and Shigeru Tachibana[2,b)]
[1]*Department of Mechanical Engineering, Tokyo University of Science, 6-3-1 Niijuku, Katsushika-ku, Tokyo 125-8585, Japan*
[2]*Japan Aerospace Exploration Agency, 7-44-1 Jindaiji-Higashimachi, Chofu-shi, Tokyo 182-8522, Japan*

(Received 13 May 2017; accepted 9 February 2018; published online 16 March 2018)

We have intensively studied the dynamic behavior of combustion instability in a cylindrical combustor with an off-center installed coaxial injector. The most interesting discovery in this study is the appearance of a deterministic chaos in a transition from a dynamically stable state to well-developed high-frequency thermoacoustic combustion oscillations with increasing the volume flow rate of nitrogen with which oxygen is diluted. The presence of deterministic chaos is reasonably identified by considering an extended version of the Sugihara-May algorithm [G. Sugihara and R. May, Nature **344**, 734 (1990)] as a local predictor and the multiscale complexity-entropy causality plane based on statistical complexity. *Published by AIP Publishing.* https://doi.org/10.1063/1.5025480

Thermoacoustic combustion oscillations possessing a rich variety of dynamic behavior, which is affected by nonlinear interactions among a turbulent flow, chemical reactions, and chamber acoustic perturbations, are induced in confined combustion systems. Their onset gives rise to serious mechanical stress, leading to the destruction of combustors. The characterization of the transition process to thermoacoustic combustion oscillations is of fundamental importance to the systemization of combustion instability. In this study, we characterize the dynamic behavior of combustion instability in a cylindrical combustor with an off-center installed coaxial injector using nonlinear time series analysis in terms of symbolic dynamics, statistical complexity, and nonlinear forecasting. Thermoacoustic combustion oscillations with a high frequency, which is strongly dominated by the first tangential mode of the combustion chamber, are clearly observed in this combustor. With increasing volume flow rate of nitrogen, with which oxygen is diluted, deterministic chaotic dynamics appears in the transition from a dynamically stable state with aperiodic and small fluctuations to well-developed thermoacoustic combustion oscillations. An extended version of the Sugihara-May algorithm[1] as a local predictor and the multiscale complexity-entropy causality plane incorporating a scale-dependent approach clearly show the possible presence of deterministic chaos prior to well-developed thermoacoustic combustion oscillations.

I. INTRODUCTION

Nonlinear time series analysis based on dynamical systems theory has potential use for extracting the deterministic features hidden in complex phenomena,[2] leading to possible new engineering applications to detect the onset of unstable phenomena. Recent advances have led to significant research to understand the nonlinearity in dynamic behavior observed in many disciplines from physics to mechanical and electrical engineering.[3] One of the authors has demonstrated the potential utility of dynamical systems theory for various physical settings including magnetohydrodynamic instability,[4] flame front instability induced by buoyancy/swirl coupling[5,6] or radiative heat loss,[7,8] and chaotic traveling waves in a falling film flow.[9]

Strong mutual coupling between heat release rate fluctuations and longitudinal/transverse acoustic modes in a pressure field through a combustion process gives rise to self-excited thermoacoustic combustion oscillations.[10] Thermoacoustic combustion oscillations are classified by combustion chamber pressure fluctuations, depending on the range of the dominant frequency in the chamber: low- (<50 Hz), intermediate- (50–1000 Hz), and high-frequency (>1000 Hz) combustion oscillations.[11] The physical mechanism underlying thermoacoustic combustion oscillations has been studied for various types of combustor,[11–13] and the characterization of the transition process to thermoacoustic combustion oscillations is of major importance in a wide range of areas in current combustion physics. Regarding the dynamic behavior in well-developed thermoacoustic combustion oscillations in a liquid rocket model combustor, linear analysis such as power spectral analysis has been performed in most studies.[14–16] This method is useful for extracting the dominant instability modes but is limited in terms of obtaining an in-depth understanding and interpretation of a rich variety of complex dynamics affected by the nonlinear interactions among a turbulent flow, chemical reactions, and chamber acoustic perturbations. Recent progress in the studies of combustion instability using nonlinear time series analysis has enabled us to encompass the understanding of quasi-periodicity, intermittency, and chaos in combustion dynamics. The correlation dimension,[17] a positive Lyapunov exponent,[18] and the recurrence quantifications[19] have mainly been used, but the characterization of combustion instability using nonlinear time series analysis still remains an open question. The correlation dimension and a positive Lyapunov exponent often lead to misinterpretation for the signature of chaos

a)Electronic mail: gotoda@se.ritsumei.ac.jp
b)Electronic mail: tachibana.shigeru@jaxa.jp

when a time series is short, temporally correlated, and/or contaminated with observational noise. Therefore, more plausible analyses from different viewpoints should be taken into account to show the possible presence of chaos.

Two of the authors[20] have recently conducted an experimental study on high-frequency combustion oscillations in a cylindrical combustor with an off-center installed coaxial injector, which is related to a liquid rocket engine model combustor. Dynamic behavior of pressure fluctuations during thermoacoustic combustion oscillations, which is dominated by the first tangential (1T) mode, reasonably corresponds to that obtained by numerical simulation.[21] They also found an interesting transition from a dynamically stable state to well-developed thermoacoustic combustion oscillations with increasing volume flow rate of nitrogen with which oxygen is diluted.

The purpose of this study is to characterize combustion instability in a cylindrical combustor with an off-center installed coaxial injector using nonlinear time series analysis in terms of symbolic dynamics, statistical complexity, and nonlinear forecasting. The concept of entropy, which can be considered as the rate of production of information, is important for treating complex nonlinear phenomena. The Shannon entropy is a well-known invariant describing the measure of disorder in a system from the viewpoint of information theory. In this study, we consider the permutation entropy[22] in terms of symbolic dynamics to quantify the randomness of combustion dynamics. It represents the Shannon entropy considering the probability distribution of possible existing rank order patterns in a time series and has been shown to provide a deep understanding of the dynamical state in a wide spectrum of physical settings.[6,9] In addition to the permutation entropy, we use the multiscale complexity-entropy causality plane incorporating a scale-dependent approach in terms of statistical complexity to distinguish deterministic dynamics from stochastic dynamics.[23] It can quantify not only the randomness of dynamics but also the degree of correlational structures. A deterministic chaotic process has the important property of short-term predictability and long-term unpredictability. On this basis, we use an extended version of the Sugihara-May algorithm[1] involving the update of library data as a local predictor, which has been shown to ensure reliable performance in distinguishing deterministic dynamics from stochastic dynamics from the viewpoint of orbital instability in a phase space.[9]

II. EXPERIMENTS

The configuration of our experimental system is shown in Fig. 1. A cylindrical combustor is identical to that used in previous studies.[20,24] The diameter and length of the combustor are 200 and 500 mm, respectively. A coaxial injector is mounted 72 mm from the center of the combustion chamber to excite tangential mode instability. The working gases are hydrogen (H_2) and oxygen (O_2) diluted with nitrogen (N_2) under atmospheric conditions. H_2 is issued from the outer injector with a diameter of 8.6 mm, while the oxidizer ($O_2 + N_2$) is issued from the inner injector with a diameter of 4.9 mm. The mass flow rate of H_2 and O_2 is 100 and 90 L/min, respectively. The mass flow rates of N_2 are gradually increased so as to induce the 1T mode instability, keeping the mass flow rates of H_2 and O_2 constant. The pressure fluctuations are measured by pressure transducers (Kulite Semiconductor Products, Model XTEL-190-15G). Pressure ports PT1-PT5 are located on the wall of the combustion chamber. The sampling frequency of the obtained time series is set to 102.4 kHz. A spatial OH* chemiluminescence intensity distribution is obtained in this study by a high-speed video camera (Photron) with 20000 frames per second, to

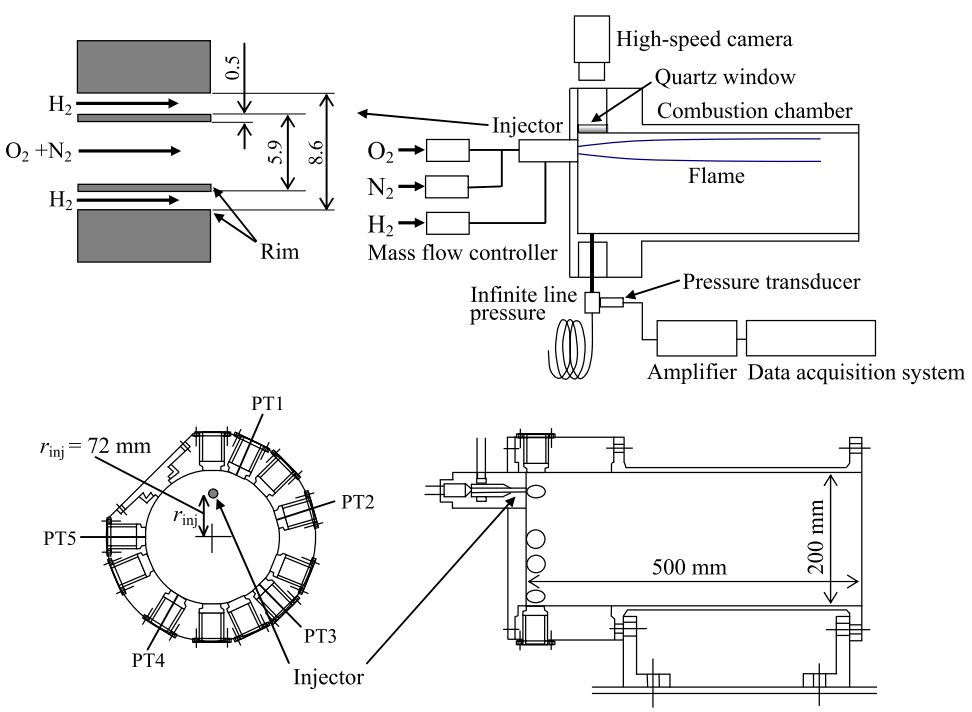

FIG. 1. Experimental apparatus.

investigate the dynamic behavior of high-frequency thermoacoustic combustion oscillations.

III. MATHEMATICAL FRAMEWORK OF ANALYTICAL METHODS

A. Nonlinear forecasting

Nonlinear forecasting method involving the update of library data enables us to clearly extract the short-term predictability and long-term unpredictability hidden in complex dynamics.[9,25] In this method, the time series of p' is first divided into two intervals, namely $t \in [0; t_L]$ and $t \in [t_L; T_f]$, and two corresponding data sets: one is used as library data to predict temporal evolutions of p' and the other is used as reference data for comparison with the predicted p'. Note that, similarly to in a previous study,[25] D-dimensional phase space[26] consisting of position vectors $\mathbf{p}(t) = (p'(t), p'(t-\tau), \ldots, p'(t-(D-1)\tau))$ is used for the nonlinear forecasting method. After finding the vectors $\mathbf{p}(t_k)(k = 1, 2, \ldots, K)$ neighboring the final vector $\mathbf{p}(t_f)$ from all position vectors in the phase space, $\mathbf{p}(t_k)$ is mapped to $\mathbf{p}(t_k + T)$ after time T, where $T = T_s \Delta t$, Δt is the sampling time of p', and T_s is a time step with arbitrary integer. We finally obtain the predicted $\hat{\mathbf{p}}(t_f + T)$ using a nonlinearly weighted sum of $\mathbf{p}(t_k + T)$.

$$\hat{\mathbf{p}}(t_f + T) = \frac{\sum_{k=1}^{K} \mathrm{e}^{-\|\mathbf{p}(t_k) - \mathbf{p}(t_f)\|} \cdot \mathbf{p}(t_k + T)}{\sum_{k=1}^{K} \mathrm{e}^{-\|\mathbf{p}(t_k) - \mathbf{p}(t_f)\|}}. \tag{1}$$

If nonlinear deterministic dynamics exists in an observed time series, short-term predictability appears in the increment process of the time series; the correlation coefficient C between the original and predicted time series for the incremental process is high at a small prediction time t_p.[25] Note that in this method involving the update of library data, t_p represents the duration of the actual temporal evolutions of p' added to the library data.

Similarly to in a previous study,[25] the time lag τ at which the mutual information I first reaches a minimum is used in this study as a suitable time lag in accordance with the prescription of Fraser and Swinney.[27] Here, I is given by

$$I = \sum_{i,j} p_{i,j} \log_2 \frac{p_{i,j}}{p_i p_j}, \tag{2}$$

where p_i is the probability density function represented by the one-dimensional histogram constructed from $p'(t)$, p_j is the probability density function represented by the one-dimensional histogram constructed from $p'(t+\tau)$, and $p_{i,j}$ is the joint probability density function represented by the two-dimensional histogram. The false nearest neighbors (FNN) method proposed by Kennel *et al.*[28] is widely applied to the optimization of the embedding dimension of a phase space. It is obtained by computing the ratio R of the Euclidean distances between the position vectors in $D+1$- and D-dimensional phase spaces, as shown in Eq. (3). The embedding dimension D when R first falls below a threshold R_{thre} (=15) in terms of D is adopted to this study as a suitable dimension.[28] We set D to 5 on the basis of FNN computations

$$R = \frac{\sqrt{d_{D+1}^2 - d_D^2}}{\sqrt{d_{D+1}^2}} > R_{thre}. \tag{3}$$

Here, d_D is the Euclidean distance between the position vector $\mathbf{p}$ and its nearest-neighbor vector in the D-dimensional phase space.

B. Multiscale complexity-entropy causality plane

Zunino *et al.*[29] reported that the multiscale complexity-causality plane (CECP) consisting of the permutation entropy and the Jensen-Shannon statistical complexity enables us to clearly distinguish between the stochastic behavior of Brownian motion and high-dimensional chaos. They reported that the multiscale CECP can robustly characterize short and noisy data sets by conducting a systematic study on the relation between additive noise and the changes in the trajectories on the CECP. In fact, the utility of the multiscale CECP has been shown in a recent experimental study on buoyancy-induced flame instability with a swirling flow[6] and dynamics of turbulent atmospheric surface layer.[30] We first estimate the permutation entropy H_p in a similar manner to in Ref. 6. In this method, after all possible permutations ($D!$ permutations) of D successive data points in time series consisting of the rank order in the components of $\mathbf{p}(t) = (p'(t), p'(t+\tau), \ldots, p'(t+(D-1)\tau))$, indexed as $\pi_j (j = 1, 2, \ldots, D!)$, are counted, the probability distribution $\mathbf{P} = p(\pi_j)(j = 1, 2, \ldots, D!)$ is given by

$$p(\pi_j) = \frac{\#\{\mathbf{p}(t_i) | i \le N - D - 1)\tau; \mathbf{p}(t_i) \text{ has type } \pi_j\}}{N - (D-1)\tau}, \tag{4}$$

where D is the embedding dimension, N is the number of data points, and # represents the realization frequency of permutation type π_j. H_p normalized by the maximum permutation entropy ($= \log_2 D!$) corresponding to a completely random process is obtained by substituting Eq. (4) into the definition of the Shannon entropy

$$H_p[\mathbf{P}] = \frac{-\sum_{\pi_j} p(\pi_j) \log_2 p(\pi_j)}{\log_2 D!}. \tag{5}$$

Note that H_p is zero for a monotonically increasing or decreasing process, while it is unity for a completely random process. On the basis of the FNN computation and a recent study,[31] D is set to 5 in this study. The Jensen-Shannon statistical complexity C_{JS} is defined as

$$C_{JS}[\mathbf{P}] = Q_{JS}[\mathbf{P}, \mathbf{P_e}] H_p[\mathbf{P}], \tag{6}$$

$$\mathbf{P_e} = \{1/D!, 1/D!, \ldots, 1/D!\}, \tag{7}$$

where $Q_{JS}[\mathbf{P}, \mathbf{P_e}]$ is the disequilibrium and is defined as the difference between $\mathbf{P}$ and the uniform distribution $\mathbf{P}_e$. $Q_{JS}[\mathbf{P}, \mathbf{P_e}]$ is given by

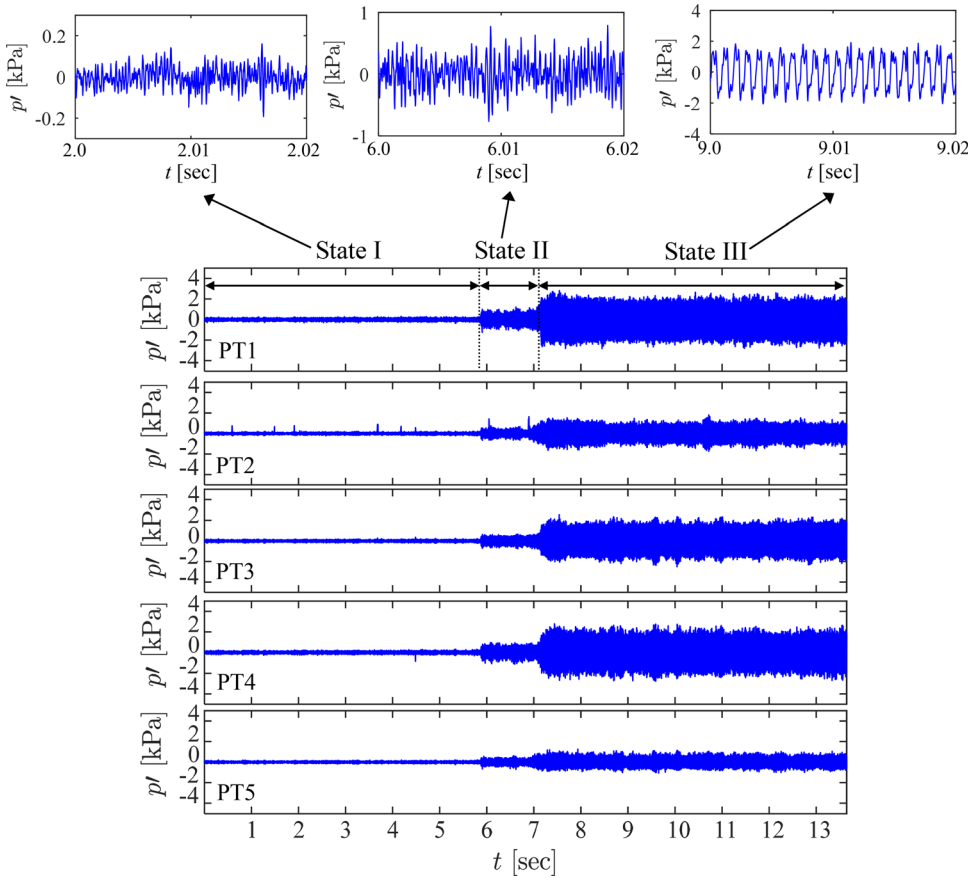

FIG. 2. Temporal evolutions of pressure fluctuations p' with increasing amount of N_2 added to the oxidizer.

$$Q_{JS}[\mathbf{P},\mathbf{P_e}] = \frac{\log_2 D!}{Q_{JS,\max}}\{H_p[(\mathbf{P}+\mathbf{P_e})/2] - H_p[\mathbf{P}]/2 - H_p[\mathbf{P_e}]/2\}, \tag{8}$$

$$Q_{JS,\max} = -\frac{1}{2}\left\{\frac{D!+1}{D!}\log_2(D!+1) - 2\log_2(2D!) + \log_2 D!\right\}. \tag{9}$$

The H_p–C_{JS} plane can quantify not only the randomness of dynamics but also the degree of correlational structures.[23] For a given value of H_p, C_{JS} can take values between a minimum of $C_{JS,\min}$ and a maximum of $C_{JS,\max}$.

IV. RESULTS

Temporal evolutions of pressure fluctuations p' are shown in Fig. 2. Irregular dynamics with small oscillation amplitudes is observed in p' during the dynamically stable state ($t < 5.8$ s). The amplitude of p' markedly increases at $t = 6$ s, indicating the sustainment of the irregularity. The combustion state finally leads to well-developed thermoacoustic combustion oscillations with large amplitude and strong periodicity. In this study, we classify these combustion states into three regimes, states I, II, and III, and focus on the pressure fluctuations at PT1 as a representative case. Note that the amplitude ratio A_2/A_1 for p' in states I and II is about 4.5, where A_1 and A_2 are the standard deviations of the pressure fluctuations for states I and II during 1 s, respectively. Figure 3 shows the changes in the formation regime of the combustion state with increasing amount of nitrogen Q_{N_2} under the condition of $Q_{H_2} = 100$ L/min. At $Q_{O_2} = 90$ L/min, we observe a significant transition from state I to state III via state II as Q_{N_2} exceeds 39.4 L/min.

Figure 4 shows temporal evolutions of the power spectrum density with increasing amount of N_2 added to the oxidizer. A dominant peak with $f = 175$ Hz is clearly formed for all states regardless of the amount of N_2. This instability mode corresponds to the 0 L mode (quarter wave) in the longitudinal direction of the combustor. An additional dominant peak with $f = 1100$ Hz appears during state III, and is generated by the 1 T mode of the combustion chamber. The presence of these modes has been confirmed in a recent numerical simulation.[21] When

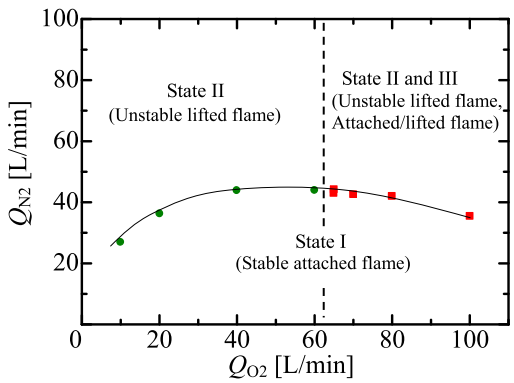

FIG. 3. Changes in formation regime of combustion state with increasing amount of nitrogen added to the oxidizer Q_{N_2}. Note that Q_{H_2} is set to 100 L/min.

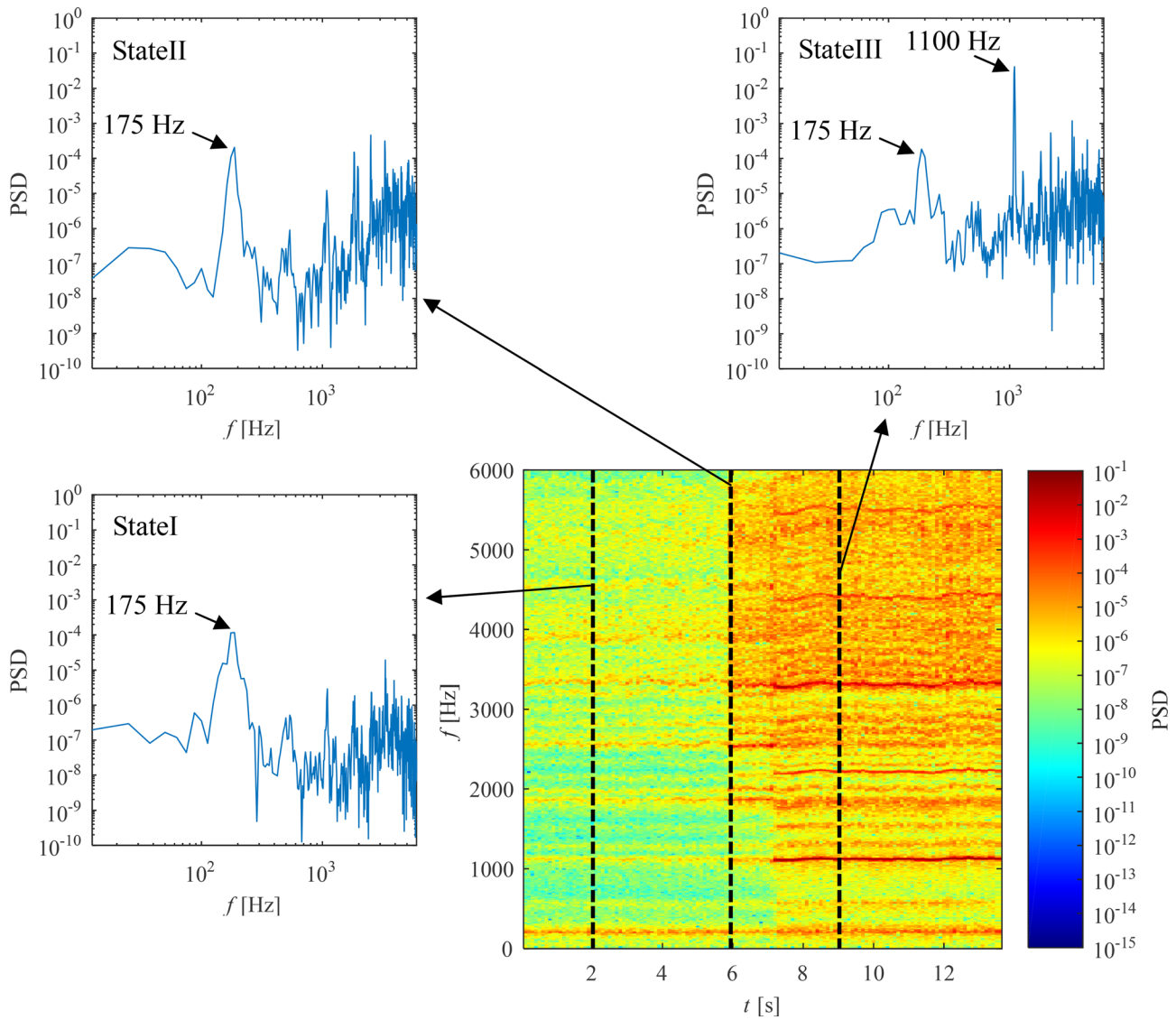

FIG. 4. Temporal evolutions of power spectrum density with increasing amount of nitrogen added to the oxidizer Q_{N_2}.

N_2 is not added to the oxidizer, the combustion field consists of two dominant flames: one is an inner diffusion flame between H_2 and O_2 jets with the attachment of flame base at the oxidizer-injector rim, and the other is an outer diffusion flame between the H_2 jet and ambient air. Dynamic behavior of these flames during state I is stable and remains nearly unchanged with the addition of a small amount of N_2. Above the critical amount rate of N_2, the inner diffusion flame base lifts from the oxidizer-injector rim, leading to state II. Temporal evolutions of OH* chemiluminescence intensity for state III are shown in Fig. 5. The five images in the first row show the flame moving downstream, while the five images in the second row show them moving upstream during one cycle of high-frequency thermoacoustic combustion oscillations. As shown in images 2 to 4, flame front moves downstream with time and the flame base in image 5 is further from the injector rim than in images 1 to 3. The flame base suddenly propagates upstream in image 7, and attaches to the injector rim in image 10. These observations correspond to those obtained by the numerical simulation.[21] The formation of state III is accompanied by two processes: the detachment of flame base from the oxidizer-injector rim and the attachment. The significant changes in heat release fluctuations owing to the periodic detachment/attachment of flame base to the oxidizer-injector rim with increasing amount of added N_2 couple strongly with the pressure fluctuations induced by the 1T mode, resulting in the formation of periodic oscillations with large amplitudes. The presence of the acoustically coupled pulsating flame dynamics is the primary driving factor inducing well-developed high-frequency thermoacoustic combustion oscillations, which is quantitatively shown using the Rayleigh index. Details of this physical mechanism are clearly identified from the numerical simulation.[21]

Variation in C in state II is shown in Fig. 6 as a function of t_p. C for p' is 0.98 for one-step-ahead prediction ($T_s = 1$) corresponding to $t_p = 9.7656 \times 10^{-6}$ s, while C for the increments $\Delta p'(= (p'(t_i + 1) - p'(t_i))$ is 0.92. The distribution of C in terms of t_p for $\Delta p'$ nearly corresponds to that for p', clearly demonstrating short-term predictability and long-term unpredictability. On the basis of Ref. 25, this indicates the presence of chaotic dynamics in state II. Variations in H_p

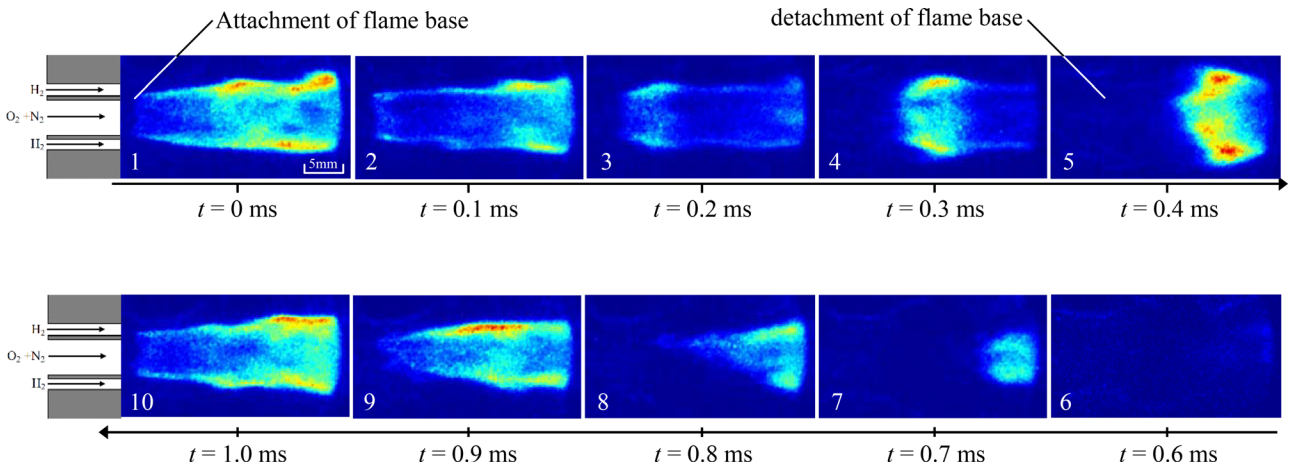

FIG. 5. Temporal evolutions of OH* chemiluminescence intensity for state III.

and C_{JS} in terms of τ are shown in Fig. 7 for states I, II, and III, together with the CECP. H_p in state I reaches a minimum value at $\tau = 2$, and C_{JS} reaches a maximum value at $\tau = 3$. The H_p–C_{JS} plane possesses a clockwise loop with increasing τ, indicating the presence of noisy-chaotic dynamics. C_{JS} in state II has a maximum value at $\tau = 2$, and H_p increases throughout this domain. The location of (H_p, C_{JS}) moves from the left-side to the right-side with a parabolic curve as τ is increased, strongly indicating the presence of deterministic chaos. These results obtained by nonlinear forecasting and multiscale CECP clearly show that deterministic chaotic dynamics exists in pressure fluctuations during state II. Note that the definition of deterministic chaos in this study is essentially based on orbital instability: short-term predictability and long-term unpredictability of trajectories in phase space. An important point to note here is that C_{JS} takes a maximum value at $\tau = 3$ for state I. It would be interesting to explore the physical process with a time scale of approximately 30 μs, corresponding to $\tau = 3$. The spatial distribution of OH* chemiluminescence intensity obtained using by a high-speed camera with a higher frame rate than 33 kHz may be needed to reveal the hidden physical process in pressure fluctuations at state I. $H_p(C_{JS})$ in state III reaches almost unity(zero) at $\tau = 93$. This value of τ corresponds to the period of the 1T mode. Zunino *et al.*[29] showed that a local maximum (minimum) of $H_p(C_{JS})$ in terms of τ periodically appears in the dynamics of a stochastically driven van der Pols oscillator producing noisy periodic oscillations. Noiray and Denisov[32] recently showed that the dynamics of thermoacoustic combustion oscillations can be described by stochastically driven Pandel Vole oscillators. Although the shape of the H_p–C_{JS} plane for state III does not coincide with that obtained by stochastically driven Pandel Vole oscillators, on these bases, it is conceivable that the dynamic behavior of pressure fluctuations in state III represents noisy periodic oscillations. Our results demonstrate that the CECP incorporating a scale-dependent approach is useful for discussing the presence of deterministic/noisy chaos in combustion states, indicating the potential use of the multiscale CECP for detecting the significant transition from state I to state III via state II.

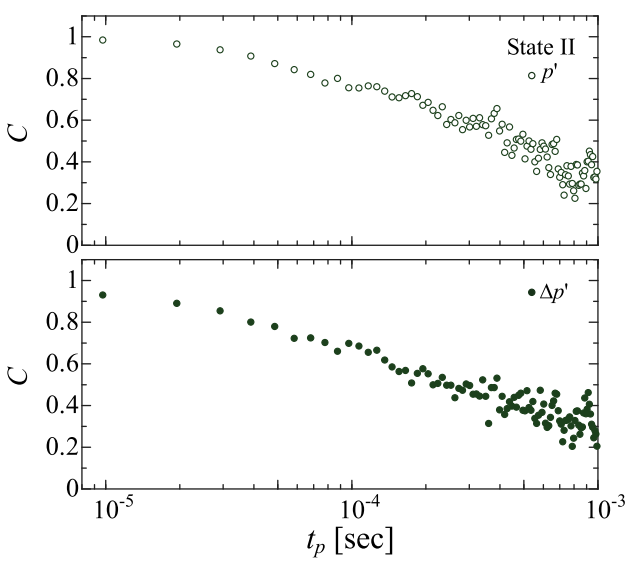

FIG. 6. Correlation coefficient C as a function of prediction time t_p in state II. The embedding dimension D is 5. Note that the embedding delay time τ is determined by the mutual information.

V. DISCUSSION

Many studies on dynamics of thermoacoustic combustion oscillations induced by the 0L mode in a confined system[25,33–40,43,44] have provided a new interpretation of combustion instability from the viewpoint of dynamical systems theory. However, a scale-dependent approach has not been introduced and nonlinear invariants have been computed at a specific embedding delay time. An advantage of the multiscale CECP is that one can distinguish chaotic processes from stochastic processes without determining a specific embedding delay time. The conventional approach considering only a single temporal scale in combination with the surrogate data method is valid for discussing the presence of nonlinear determinism, but the multiscale CECP is important for treating the transition process to well-developed high-frequency thermoacoustic combustion oscillations dominated by the 1T mode. As reported by Zunino *et al.*,[29] the multiscale CECP is useful

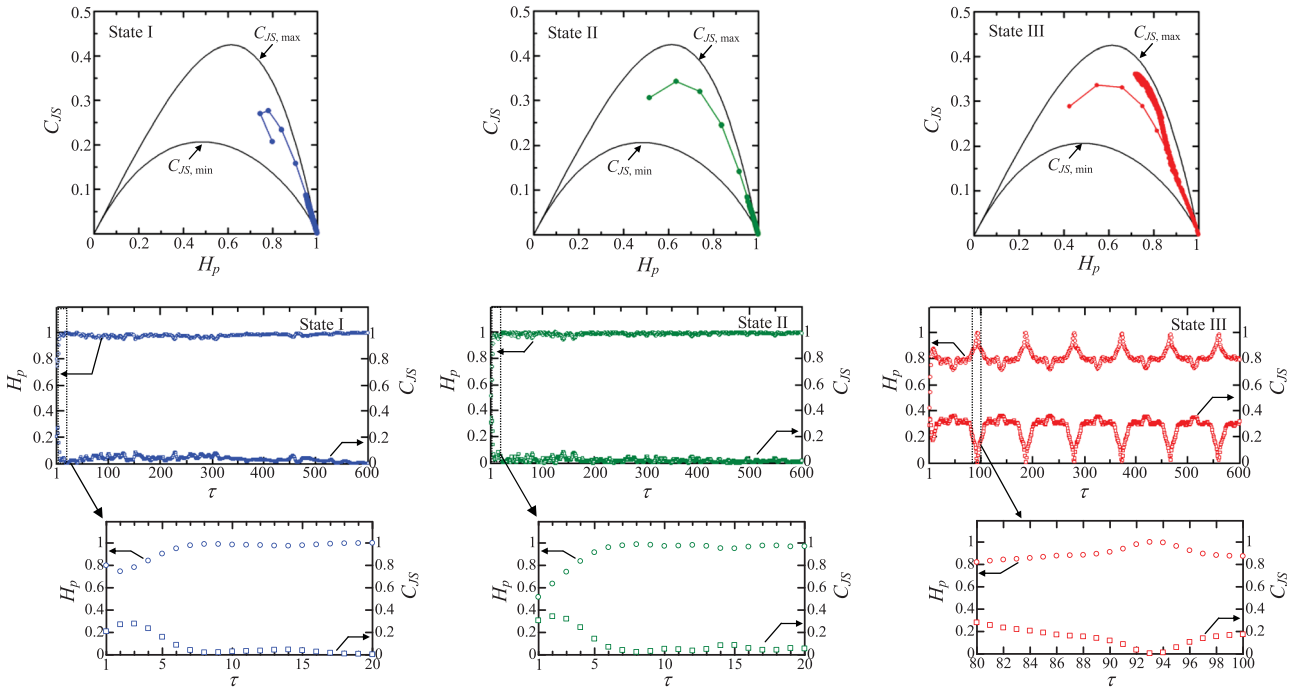

FIG. 7. Variations in permutation entropy H_p and Jensen-Shannon statistical complexity C_{JS} in terms of the embedding delay time τ for states I, II, and III, together with the complexity-entropy causality plane.

for extracting the intrinsic chaotic nature in time series, but we should keep in mind that the presence of a maximum for C_{JS} in terms of H_p on the CECP is a necessary but not sufficient condition for giving evidence for the presence of chaos.

The characterization of the transition process to thermoacoustic combustion oscillations and the opposite transition process using nonlinear time series analysis in terms of dynamical systems theory and complex networks has been conducted in many previous studies.[37,38,40,41] These studies mainly dealt with a turbulent premixed flame using two types of rectangular combustor: one was a swirled-stabilized type and the other was a bluff-body type forming a large-scale recirculation flow. They reported the appearance of thermoacoustic combustion oscillations dominated by the 0L mode with a intermediate-frequency of around 200 Hz. In the previous studies[25,35,36,39,42] using a swirl-stabilized type combustor, the entire flow field inside the combustion chamber was mainly composed of two large-scale recirculation regimes: a vortex breakdown bubble generated by a swirling flow, and an outer recirculation flow in a dump plate generated by the backward-facing step flow. The entire flame during thermoacoustic combustion oscillations with intermediate-frequency of around 200 Hz was sustained by both recirculation regions, with the roll up of turbulent premixed flame due to vortical structures stemming from the convective interaction in the shear layers. Here, we deal with a turbulent inverse diffusion flame using a cylindrical combustor without a flame holder such as a swirler or bluff-body. In addition, thermoacoustic combustion oscillations dominated by the 1T mode with a frequency higher than 1000 Hz are clearly formed in the cylindrical combustor without large-scale recirculation flows (note that our study using H_2/O_2 as a fuel/oxidizer is related to combustion instability in a liquid rocket engine model combustor). As shown in Fig. 5, the formation of high-frequency thermoacoustic combustion oscillations is accompanied by the periodic detachment/attachment of the flame base to the oxidizer-injector rim, which corresponds to the recent numerical studies by Matsuyama *et al.*[21] Therefore, the observed transition phenomena to high-frequency thermoacoustic combustion oscillations essentially differs from the previous studies dealing with intermediate-frequency combustion oscillations in a swirl-stabilized type combustor.[25,35,36,39,42] Nair and co-workers[43,44] recently obtained a useful deterministic model describing a significant transition from combustion noise to thermoacoustic combustion oscillations induced by the 0L mode via intermittency in a bluff-body stabilized combustor. Nonlinear dynamical systems based on the physical mechanism we presented here will be desirable for obtaining a more comprehensive understanding of the observed dynamics. The characterization of combustion dynamics generated by the above mechanism is of great importance, and in this work we focused on revealing the dynamic behavior of combustion instability from the viewpoints of symbolic dynamics, statistical complexity, and nonlinear forecasting. We were able to demonstrate the presence of noisy-chaos, deterministic chaos, and a noisy periodic oscillations in pressure fluctuations, showing the possible prediction of the precursor of thermoacoustic combustion oscillations. Finally, note that the presence of chaotic dynamics depends on the resolution of time series observed in an actual system.[45] It would be of fundamental and practical importance to the combustion community to study whether or not the resolution of the pressure sensor affects the detection of chaos.

VI. SUMMARY

We have intensively studied the dynamic behavior of combustion instability in a cylindrical combustor with an off-center installed coaxial injector. With increasing volume flow rate of nitrogen, with which oxygen is diluted, deterministic chaotic

dynamics appears in the transition from a dynamically stable state with aperiodic and small fluctuations to well-developed high-frequency thermoacoustic combustion oscillations. An extended version of the Sugihara-May algorithm[1] as a local predictor and the multiscale complexity-entropy causality plane incorporating a scale-dependent approach clearly show the possible presence of deterministic chaos prior to well-developed thermoacoustic combustion oscillations. Spatial distribution of OH* chemiluminescence intensity shows that the formation of high-frequency thermoacoustic combustion oscillations is accompanied by the periodic detachment/attachment of the flame base to the oxidizer-injector rim.

ACKNOWLEDGMENTS

One of the authors (H.G.) was partially supported by a Grant-in-Aid for Scientific Research (B).

[1]G. Sugihara and R. May, Nature **344**, 734 (1990).
[2]H. Kantz and T. Schreiber, *Nonlinear Time Series Analysis* (Cambridge University Press, 1997).
[3]M. Small, *Applied Nonlinear Time Series Analysis* (World Scientific, 2005).
[4]H. Gotoda, R. Takeuchi, Y. Okuno, and T. Miyano, J. Appl. Phys. **113**, 124902 (2013).
[5]H. Gotoda, T. Miyano, and I. G. Shepherd, Phys. Rev. E **81**, 026211 (2010).
[6]H. Gotoda, H. Kobayashi, and K. Hayashi, Phys. Rev. E **95**, 022201 (2017).
[7]H. Gotoda, T. Ikawa, K. Maki, and T. Miyano, Chaos **22**, 033106 (2012).
[8]H. Kinugawa, K. Ueda, and H. Gotoda, Chaos **26**, 033104 (2016).
[9]H. Gotoda, M. Pradas, and S. Kalliadasis, Int. J. Bifurcation Chaos **25**, 1530015 (2015).
[10]J. O'Connor, V. Acharya, and T. C. Lieuwen, Prog. Energy Combust. Sci. **49**, 1 (2015).
[11]T. C. Lieuwen and V. Yang, *Combustion Instabilities in Gas Turbine Engines: Operational Experience, Fundamental Mechanisms and Modeling*, Progress in Astronautics and Aeronautics Vol. 210 (American Institute of Aeronautics and Astronautics, 2005).
[12]T. C. Lieuwen, *Unsteady Combustor Physics* (Cambridge University Press, 2012).
[13]V. Yang and W. Anderson, *Liquid Rocket Engine Combustion Instability*, Progress in Astronautics and Aeronautics Vol. 169 (American Institute of Aeronautics and Astronautics, 1995).
[14]L. Selle, R. Blouquin, M. Theron, L. H. Dorey, M. Schmid, and W. E. Anderson, J. Propul. Power **30**, 978 (2014).
[15]F. Richecoeur, P. Scouflaire, S. Ducruix, and S. Candel, J. Propul. Power **22**, 790 (2006).
[16]M. E. Harvazinski, W. E. Anderson, and C. L. Merkle, J. Propul. Power **29**, 396 (2013).
[17]P. Grassberger and I. Procaccia, Phys. Rev. Lett. **50**, 346 (1983).
[18]H. Kantz, Phys. Lett. A **185**, 77 (1994).
[19]N. Marwan, M. Carmenromano, M. Thiel, and J. Kurths, Phys. Rep. **438**, 237 (2007).
[20]S. Yoshida, S. Tachibana, K. Shimodaira, T. Shimizu, D. Hori, S. Matsuyama, J. Shinjo, Y. Mizobuchi, and K. Kobayashi, in *Proceedings of the 47nd Combustion Symposium of Japan* (2009), p. 231.
[21]S. Matsuyama, D. Hori, T. Shimizu, S. Tachibana, S. Yoshida, and Y. Mizobuchi, J. Propul. Power **32**, 628 (2016).
[22]C. Bandt and B. Pompe, Phys. Rev. Lett. **88**, 174102 (2002).
[23]O. A. Rosso, H. A. Larrondo, M. T. Martin, A. Plastino, and M. A. Fuentes, Phys. Rev. Lett. **99**, 154102 (2007).
[24]T. Shimizu, S. Tachibana, S. Yoshida, D. Hori, S. Matsuyama, and Y. Mizobuchi, AIAA J. **49**, 2272 (2011).
[25]H. Gotoda, Y. Okuno, K. Hayashi, and S. Tachibana, Phys. Rev. E **92**, 052906 (2015).
[26]F. Takens, *Dynamical Systems of Turbulence*, Lecture Notes in Mathematics Vol. 898 (Springer-Verlag, 1981).
[27]A. M. Fraser and H. L. Swinney, Phys. Rev. A **33**, 1134 (1986).
[28]M. B. Kennel, R. Brown, and H. D. I. Abarbanel, Phys. Rev. A **45**, 3403 (1992).
[29]L. Zunino, M. C. Soriano, and O. A. Rosso, Phys. Rev. E **86**, 046210 (2012).
[30]Q. L. Li and Z. T. Fu, Phys. Rev. E **89**, 012905 (2014).
[31]C. W. Kulp and L. Zunino, Chaos **24**, 033116 (2014).
[32]N. Noiray and A. Denisov, Proc. Combust. Inst. **36**, 3843 (2016).
[33]L. Kabiraj, A. Saurabh, P. Wahi, and R. I. Sujith, Chaos **22**, 023129 (2012).
[34]K. Kashinath, I. C. Waugh, and M. P. Juniper, J. Fluid Mech. **761**, 399 (2014).
[35]H. Gotoda, H. Nikimoto, T. Miyano, and S. Tachibana, Chaos **21**, 013124 (2011).
[36]H. Gotoda, M. Amano, T. Miyano, T. Ikawa, K. Maki, and S. Tachibana, Chaos **22**, 043128 (2012).
[37]V. Nair, G. Thampi, S. Karuppusamy, S. Gopalan, and R. I. Sujith, Int. J. Spray Combust. Dyn. **5**, 273 (2013).
[38]V. Nair, G. Thampi, and R. I. Sujith, J. Fluid Mech. **756**, 470 (2014).
[39]H. Gotoda, Y. Shinoda, M. Kobayashi, Y. Okuno, and S. Tachibana, Phys. Rev. E **89**, 022910 (2014).
[40]J. Tony, E. A. Goparakrishnan, E. Sreelekha, and R. I. Sujith, Phys. Rev. E **92**, 062902 (2015).
[41]M. Murugensa and R. I. Sujith, J. Fluid Mech. **772**, 225 (2015).
[42]H. Gotoda, H. Kinugawa, R. Tsujimoto, S. Domen, and Y. Okuno, Phys. Rev. Appl. **7**, 044027 (2017).
[43]V. Nair and R. I. Sujith, Proc. Combust. Inst. **35**, 3193 (2015).
[44]A. Seshadri, V. Nair, and R. I. Sujith, Combust. Theory Modell. **20**, 441 (2016).
[45]M. Cencini, M. Falcioni, E. Olbrich, H. Kantz, and A. Vulpiani, Phys. Rev. E **62**, 427 (2000).